Engineering Structures 317 (2024) 118702

Contents lists available at ScienceDirect

Engineering Structures

journal homepage: www.elsevier.com/locate/engstruct

Structural nonlinear seismic time-history response prediction of urban-scale reinforced concrete frames based on deep learning

Chenyu Zhang [a,b], Weiping Wen [a,b,*], Changhai Zhai [a,b,*], Jun Jia [c], Bochang Zhou [d,e]

[a] Key Lab of Structures Dynamic Behavior and Control of the Ministry of Education, Harbin Institute of Technology, Harbin 150090, China
[b] Key Lab of Smart Prevention and Mitigation of Civil Engineering Disaster of the Ministry of Industry and Information Technology, Harbin Institute of Technology, Harbin 150090, China
[c] The Architectural Design and Research Institute of Harbin Institute of Technology Co., Ltd., Harbin 150090, China
[d] Shanghai Earthquake Agency, Shanghai, China
[e] Shanghai Sheshan National Geophysical Observatory, Shanghai, China

ARTICLE INFO

Keywords:
Seismic time-history response prediction
Reinforced concrete frames
Easy-getting structural parameters
Urban-scale seismic response analysis
Deep learning

ABSTRACT

Efficiently predicting the seismic response of urban building clusters is essential for preemptively identifying potential seismic hazards prior to an earthquake and optimizing resource allocation post-event. However, complete information of buildings at a city scale is generally un-accessible or non-existent. Existing methods struggle to reconcile low information demands, high computational accuracy, and computational efficiency. This paper proposes a fast prediction method for structural seismic time-history responses that combines deep learning methods with easy-getting structural parameters at an urban scale. An end-to-end network with adaptive multilevel fusion output is designed, which incorporates the autoencoder concept for predicting the structural seismic time-history responses based on ground motions records and five easy-getting structural parameters. The models are compared and optimized considering the training hyperparameters and network architecture, resulting in an optimized model with low complexity that provides valuable reference values for structural seismic response. Besides, the proposed model is applied to four actual buildings with different construction time, occupancy types, and floor sizes, demonstrating its good prediction performance and significant computational advantages comparing to the universally used MDOF method.

1. Introduction

Earthquakes are a significant source of risk that jeopardizes human life and safety, as well as the safety of urban buildings, causing extensive casualties and economic losses over the past century. In this regard, the digital twin of urban building clusters has the potential to serve as a powerful tool for post-earthquake damage assessment and recovery, as well as pre-earthquake detection of seismically weak buildings. To this end, these models must be capable of swiftly and accurately calculating responses under seismic excitation. Currently, nonlinear dynamic analysis method has become the most prevailing and accurate technique for structural seismic response analysis. It starts with the selection of suitable ground motion time histories, and establishes the structural dynamic equations under ground motion excitation for a detailed structural finite element dynamic calculation model, and then solves the equations numerically, where the calculated results include the displacement, velocity and acceleration response of each degree of freedom in the structure at each moment, and the sequence of structural cracking or yielding [1]. Although this method can effectively and accurately simulate the response of structures under seismic excitation, it has some notable limitations, such as high information requirements, modeling effort, and computational costs, which are especially evident when performing analyses of urban-scale buildings.

In recent years, machine learning methods, especially deep learning methods, have witnessed a rapid development, attracting significant attention from various fields due to their remarkable capability to handle highly complex problems with high accuracy and efficiency [2, 3]. There have been many studies applying machine learning (ML) methods to the field of structural seismic response analysis for predicting structural damage states, peak responses, and time history responses, as

* Corresponding authors at: Key Lab of Structures Dynamic Behavior and Control of the Ministry of Education, Harbin Institute of Technology, Harbin 150090, China.

E-mail addresses: wenweiping@hit.edu.cn (W. Wen), zch-hit@hit.edu.cn (C. Zhai).

https://doi.org/10.1016/j.engstruct.2024.118702
Received 1 December 2023; Received in revised form 25 March 2024; Accepted 25 July 2024
Available online 30 July 2024
0141-0296/© 2024 Elsevier Ltd. All rights are reserved, including those for text and data mining, AI training, and similar technologies.

shown in Table 1.

1) Applying machine learning for seismic damage state prediction. In terms of predicting the seismic damage state of a single structure, some researchers use artificial neural networks (ANN) [4–7] to develop the predictive models of damage index or damage state for Reinforced Concrete (RC) buildings. For urban-scale buildings, related studies use adaptive neuro-fuzzy inference system (ANFIS) [8], convolutional neural network (CNN) [9,10], long short-term memory networks (LSTM) [11] to predict the earthquake damage state of a specific urban-scale building clusters based on ground motions time histories or the time-frequency distribution graphs of the earthquake records.

2) Applying machine learning for seismic peak response prediction. Existing studies have been conducted for the RC frames[12], RC buildings with different wall arrangements [13], multi-story and high-rise reinforced concrete buildings [14,15], planar steel moment frames [16], non-ductile and concentrically braced frames [17], subway stations [18], single-degree-of-freedom (SDOF) systems with different hysteresis models [19–21] or simplified multi-degree-of-freedom (MDOF) system [22], using ANN, weighted least squares support vector machine (WWLSSVM) [15], deep neural network (DNN) or CNN to predict peak displacements, peak velocities, peak floor accelerations, or peak inter-story drift ratio of structures under seismic excitation.

3) Applying machine learning for structural seismic time-history response prediction. Related studies build ANN [23], deep neural networks (DNN) [24], functional link neural networks (FLNNs) [25], locally weighted least-squares support vector machines for regression (LWLS-SVMR) [26], CNN[27–29], LSTM[30–33], recurrent neural networks (RNN) [34], convolutional LSTM networks (ConvLSTM)[35], time delay neural networks (TDNN) [36], Runge-Kutta RNN (RKRNN) [37], physics-informed multi-LSTM networks (PhyLSTM)[38], Physics-guided CNN (PhyCNN)[39], physics-based RNN model[40], discrete Physics-DNN hybridized integration time-stepper based on residual network (ResNet) [41], Physics-Informed Deep Learning model [42], Physics-informed deep 1D CNN [43], physics knowledge-based transfer learning (Phy-KTL) neural networks [44], and generative adversarial networks (GAN) [45] to predict structural responses of MDOF systems or RC buildings under seismic excitation. In addition, the randomness of ground motions and structural parameters is considered when using machine learning for seismic time-series response prediction [46,47].

The above study demonstrates the powerful capability of machine learning and the promising application in the prediction of seismic response of civil engineering structures. However, from the perspective of serving the prediction of seismic response of actual building complexes, the above studies have the following shortcomings:

1) In contrast to the peak seismic response of the buildings, the response time histories contain more information on the time-varying performance of a structure throughout the seismic process, which contributes to a more comprehensive understanding of the dynamic behavior of the structure, frequency spectrum analysis, and evaluation of dynamic parameters. Moreover, overly simplified structural analysis models (such as SDOF nonlinear systems [19–21,48]) and simplified analytical techniques (such as capacity spectrum method [8], and modal response spectrum analysis method [14]) are inadequate for capturing the nonlinear structural time-history response at individual floors within buildings.
2) Buildings with different attribute data can also greatly influence their seismic responses, and the differences in seismic performance among different buildings need to be reflected in the urban-scale seismic analysis to identify seismically weak buildings. For the current research on predicting structural seismic response time histories, the models developed in these papers aim to establish a mapping relationship between structural seismic responses and seismic ground motions using various algorithms, while the influence of structural parameters (such as building height and plan

Table 1
List of literature regarding structural seismic response analysis with ML methods (Only the latest literature on seismic time-history response prediction is listed.).

	Year	Author	Prediction Task	Algorithm
Seismic damage state prediction	2009	De Lautour et al. [4]	Structural damage of RC frames	ANN
	2017	Morfidis et al. [5]	Seismic damage state of RC buildings	ANN
	2019	Morfidis et al. [6]	Seismic damage level of RC buildings	ANN
	2020	Hansapinyo et al.[8]	Damage of buildings at urban scale	ANFIS
	2020	Xu et al. [11]	Real-time regional seismic damage assessment	LSTM
	2021	Hait et al. [7]	Global damage index (GDI) of RC buildings	ANN
	2021	Xiong et al. [9]	Damage Assessment of RC Frame Buildings after earthquakes	CNN
	2021	Lu et al. [10]	Regional post-event seismic damage assessment	CNN
Seismic peak response prediction	2010	Arslan[13]	Performance level of RC buildings	ANN
	2016	Suryanita et al. [14]	Structural responses of multi-story and high-rise RC buildings	ANN
	2017	Doran et al. [17]	Peak inter-story drift ratio of braced buildings	ANN
	2019	Gharehbaghi et al.[15]	Inelastic seismic response of RC frame structures	WWLSSVM, ANN
	2019	Kim et al. [19]	Responses of SDOF systems with different hysteresis models	CNN
	2020	Kim et al. [20]	Probabilistic evaluation of seismic responses	CNN, DNN
	2020	Oh et al. [22]	Response of simplified multi-degree-of-freedom (MDOF) system	ANN
	2021	Nguyen et al. [16]	Maximum top and inter-story drifts of planar steel moment frames	ANN, XGBoost
	2022	Kim et al. [21]	Responses of hysteretic systems having degradation and pinching	DNN
	2022	Wen et al. [12]	Seismic response prediction of RC frames	CNN
Seismic time-history response prediction	2012	Lagaros et al. [23]	One-step ahead response prediction of nonlinear buildings	ANN
	2018	Sahoo et al. [25]	Structural response of different floors of multistorey shear buildings	FLNNs
	2019	Wu et al. [27]	Structural Dynamic Response Estimation and System Identification	CNN
	2019	Zhang et al. [30]	Nonlinear structural seismic response prediction	LSTM
	2020	Oh et al. [28]	Displacement responses of building structures	CNN
	2020	Yu et al. [34]	Structural dynamics simulation	RNN, MLP

(continued on next page)

Table 1 (*continued*)

2020	Zhang et al. [38]	Seismic response modeling	Physics-informed multi-LSTM
2020	Zhang et al. [39]	Metamodeling of nonlinear structural systems	Physics-guided CNN
2021	Torky et al. [35]	Nonlinear multi-component seismic responses of structural buildings	ConvLSTM
2021	Sadeghi et al. [40]	Nonlinear structural response modeling and prediction	Physics-based RNN
2021	Fan et al. [45]	Structural dynamic response reconstruction	GAN
2022	Luo et al. [26]	Seismic response prediction of RC frames	LWLS-SVMR
2022	Xu et al. [31]	Nonlinear structural seismic response	LSTM
2022	Zhang et al. [36]	Seismic Response Meta-model of High-Rise Fame Structure	TDNN
2022	Wang et al. [46]	Probabilistic seismic response prediction of three-dimensional structures	Bayesian CNN
2022	Nikolopoulos et al.[47]	Transient analysis of stochastic nonlinear structures	1D CNN, CAE
2023	Parida et al. [24]	Surrogate modeling of non-linear structures	DNN, SVR, RF, DT
2023	Damikoukas et al.[29]	Amplitude and phase spectrograms of earthquake-induced responses	CNN
2023	Chou et al. [32]	Story drift time series and damage level estimation of buildings	LSTM
2023	Wang et al. [37]	Seismic response prediction of structures	RKRNN
2023	Guo et al. [41]	Nonlinear structural seismic response prediction	Physics-DNN hybridized integration time-stepper
2023	Zhou et al. [42]	Time history responses of multiple nodes within a specific structure	Phy-Seisformer model
2024	Bailey et al. [33]	Seismic response prediction of nonlinear steel moment resisting frame structures	LSTM
2024	Xiong et al. [43]	Extended state space fusion for seismic response modeling	Physics-informed deep 1D CNN
2024	Hu et al. [44]	Transfer learning between buildings for seismic response prediction	Phy-KTL neural networks

Abbreviations: Adaptive neuro-fuzzy inference system (**ANFIS**), Artificial neural networks (**ANN**), Convolutional autoencoders (**CAE**), Convolutional neural network (**CNN**), Convolutional long short-term memory networks (**ConvLSTM**), Deep neural networks (**DNN**), Decision trees (**DT**), Functional link neural networks (**FLNNs**), Locally weighted least-squares support vector machines for regression (**LWLS-SVMR**), Long short-term memory networks (**LSTM**), Physics knowledge-based transfer learning (**Phy-KTL**), Random forest (**RF**), Runge-Kutta recurrent neural networks (**RKRNN**), Recurrent neural networks (**RNN**), Support vector regression (**SVR**), Time delay neural networks (**TDNN**), Weighted least squares support vector machine (**WWLSSVM**).

dimensions) on this mapping relationship is not considered. Consequently, the models need to be retrained based on the corresponding data when there are differences between the application building objects and the buildings studied in these papers (such as different number of floors), which makes existing methods difficult to apply to earthquake response prediction for city-scale buildings.

3) As a prominent source of building data (like location, height, shape, etc.) for regional earthquake simulation [49–51], the present GIS data does not include the necessary data like structural skeleton and material properties [52], and the data quality and distribution details are inconsistent in different regions from open-source data like OpenStreetMap [53]. However, in studies where building information can be considered as the input, some input building parameters are difficult to obtain directly, like natural periods [9,15,22], spectral acceleration [14,16], modulus of elasticity [4,46,47], non-linear features from structural components [17,21] and resonance area [22].

In order to overcome the above drawbacks, some works are done in this study to improve the performance and practical usability in terms of the deep learning network architecture, structural parameters of inputs, and the dataset. 1). In the proposed deep learning network based on the end-to-end convolutional autoencoder architecture, the seismic time-history responses of each floor in the structures are utilized as the output, while the ground motion time history is employed as one of the two inputs, and limited structural information serves as the other input. 2). Taking into account the accessibility of building information for urban scale analysis, the height, number of stories and structural geometric configurations directly obtained from the GIS database [8,49,51,53] are used as part of the structural information inputs, and the seismic design intensity of buildings obtained from the seismic ground motion parameters zonation map of China [54] is used as the structural information inputs. 3). Moreover, the data set is derived from the seismic response results of detailed finite element models of multiple real typical buildings and contains many nonlinear response samples. To sum up, in comparison to prior studies, our deep learning model, trained on the seismic response database of fine-grained numerical models of RC frames, can swiftly give informative values of structural seismic time-history responses considering accessible structural parameters and ground motion time series, and then serve seismic damage prediction and analysis of RC frame buildings at urban scale.

The main contents of this study are organized as follows. In Section 2, the framework of proposed approach and the architecture of the basic deep learning model are introduced. The details of deep learning network training and evaluation are introduced in Section 3. Then in Section 4, the optimized model is applied to four actual buildings and the prediction performance is compared with the simplified MDOF model.

2. Proposed approach and basic network configuration

2.1. Proposed approach

The proposed approach contains two stages: offline preparation and online inference, and the whole framework is shown in Fig. 1. During the phase of offline preparation, a structural seismic response database is formed by collecting data from papers and real scenarios or computing by numerical methods, and then deep learning methods are used to build basic surrogate models and perform model comparison and optimization.

In the online inference phase, the easily accessible parameters of the target buildings are obtained from open-source GIS data (like OpenStreetMap and Google Earth), and the ground motions are selected. Subsequently, the data are preprocessed and input into the trained model to obtain the structural seismic time-history responses, which can be further carried out to assess structural damages and reconstruct

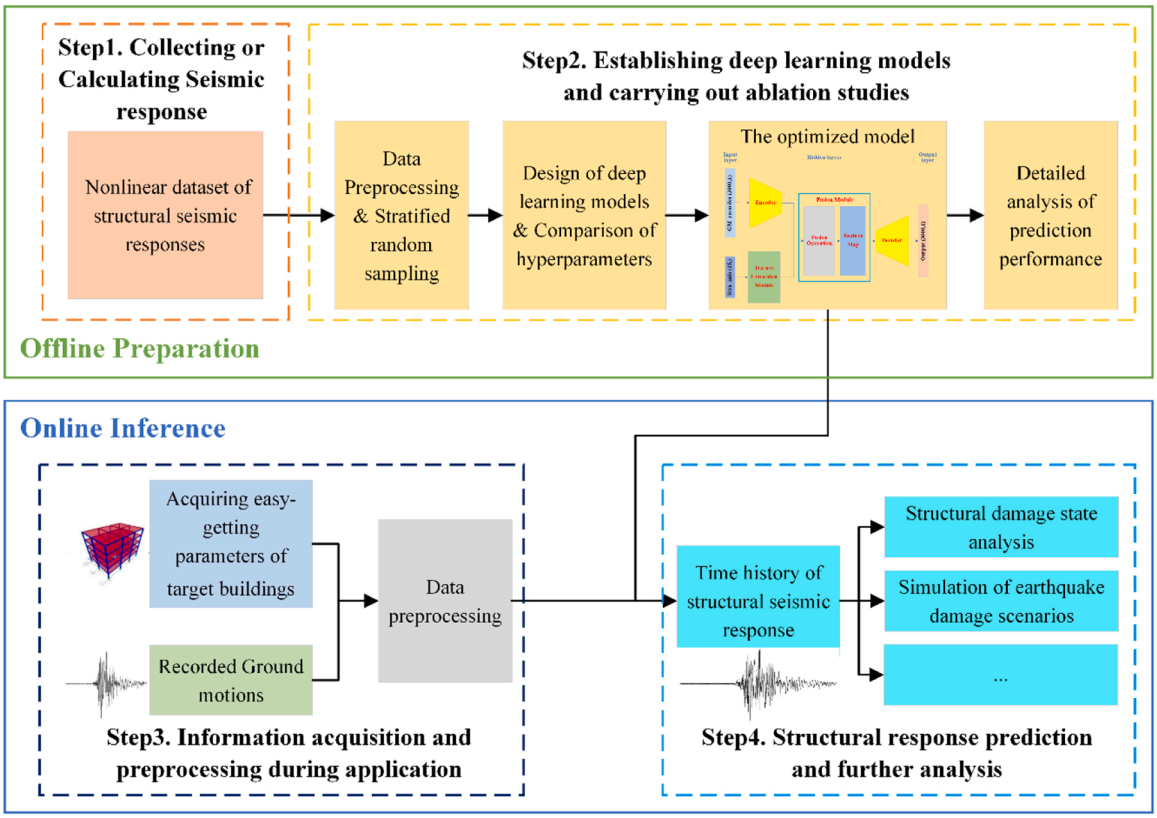

Fig. 1. Proposed approach to predict seismic time-history responses.

seismic damage scenarios.

2.2. Feasibility of applying this approach for urban-scale buildings

When applying the approach proposed in this paper to urban building clusters, the key lies in obtaining the building information of the target buildings and identifying the buildings that fall within the scope of this paper's application (low-rise to mid-rise regular RC frame structures).

For open-source GIS platforms, OpenStreetMap provides rough building footprints, structural parameters (such as number of floors and height), and geographical coordinates [53]. Google Earth offers high-resolution building satellite images for most global regions at a sub-meter level, aiding in refining rough building footprints and further calibrating necessary parameters (such as building height and number of floors) [55]. Seismic design intensity information can be directly obtained from the seismic ground motion parameters zonation map of China [54] based on coordinate information. These pieces of information already meet the structural information requirements for input into the model proposed in this paper.

It is worth noting that, due to the lack of structural type information in these open-source data sets, there is a need to infer the structural types in practical applications [56]. Xu et al. [57] analyzed data for 230,683 buildings in Tangshan City and utilized a multi-classification model in machine learning to predict building structural types by number of floors, floor height, building age, and footprint area, and the overall prediction accuracy achieved nearly 95 %.

Furthermore, governments in various countries possess varying degrees of information about urban building clusters. Taking China as an example, from 2020 to 2023, massive data on the spatial locations and physical attributes of all buildings in China were obtained through a comprehensive survey [58]. If these data are made available in the future, it would be entirely feasible to select structures that meet the research scope of this paper and directly input relevant structural information into the proposed model for seismic response prediction.

2.3. Network configuration

An autoencoder is an unsupervised neural network model that automatically learns data features through an encoding-decoding process [59,60]. Convolutional networks exhibit commendable performance in extracting features from seismic motion data [61,62], and the autoencoder architectures based on convolutional networks are widely used in transient analysis of nonlinear structures [47] and prediction of peak structural seismic responses [12]. In this paper, an end-to-end network is built combining the idea of autoencoders with multiple inputs (ground motion series and the vectorized structural information) and single output (time series of structural acceleration), where the vectorized structural information is obtained by preprocessing the five key structural parameters (i.e., seismic design intensity, number of stories, story height, longitudinal column spacing, and total transverse span) and adding a vector indicating the specific output floor of the building. The basic network architecture is shown in Fig. 2.

Specifically, the network consists of four modules:

1. **Encoder**: extracts features from the ground motion series.
2. **Feature Extraction Module**: extracts and reconstructs features from the input structural information.
3. **Fusion Module**: fuses structural features with ground motion features and maps the fused feature vector to the structural response feature vector.
4. **Decoder**: reconstructs structural time-history responses given the structural response feature vector. The Decoder is mirrored according to the encoder module to obtain the dimensionality of the target structure response.

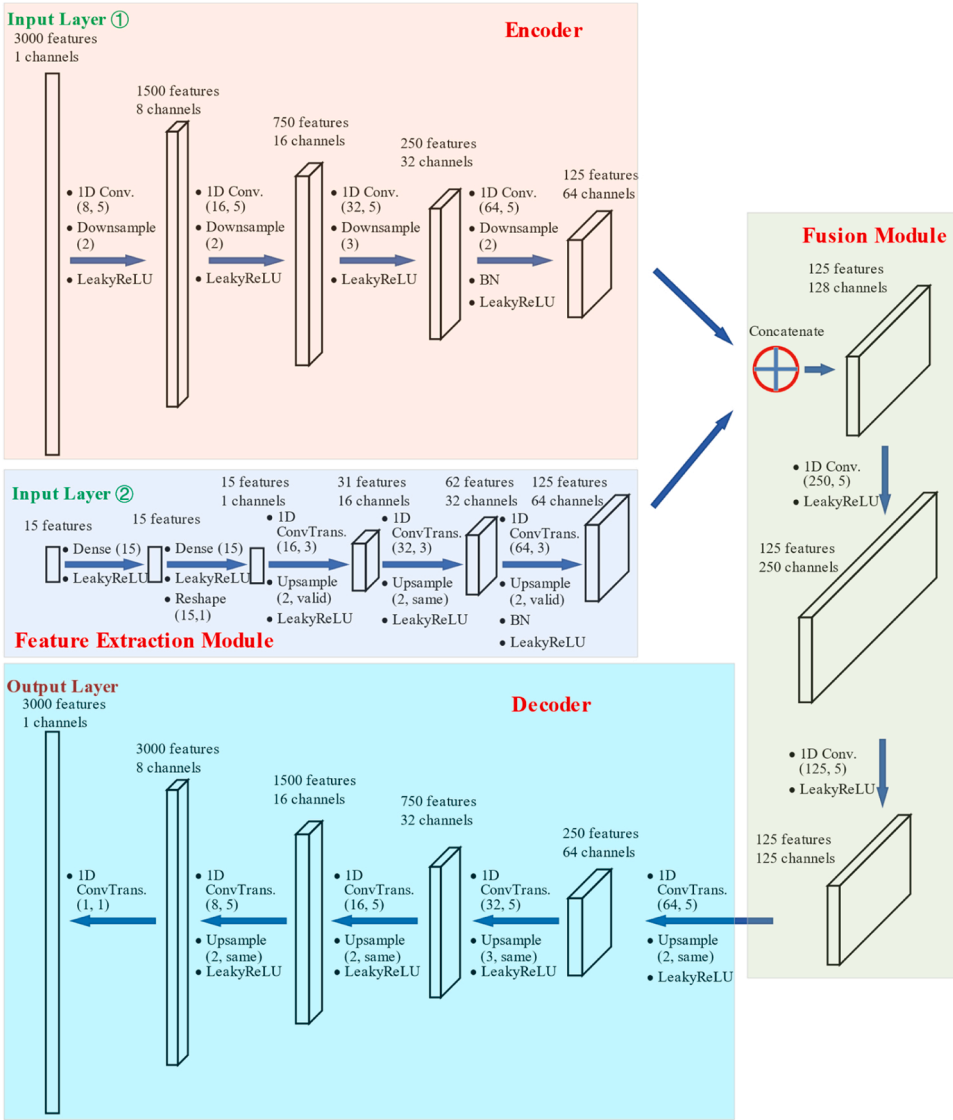

Fig. 2. The architecture of the basic model. Note: In the diagram, "**1D Conv (16, 5)**" signifies a 1D convolution layer with 16 filters and a kernel size of 5. "**Downsample (2, same)**" denotes the downsampling process with a stride of 2 and equal padding on both sides ('same' padding). The activation layer "**LeakyReLU**" employs the Leaky version of the Rectified Linear Unit. The abbreviation "**BN**" corresponds to the Batch Normalization layer. "**Dense (15)**" represents a regular densely connected neural network layer with 15 units. "**1D ConvTrans (32, 5)**" corresponds to a transposed 1D convolution layer with 32 filters and a kernel size of 5. "**Upsample (2, same)**" indicates the upsampling process with a stride of 2 and padding set to 'same', ensuring equal padding on both sides. "**Upsample (2, valid)**" signifies the upsampling process with a stride of 2 and no padding ('valid' padding). "**Concatenate**" refers to the layer that concatenates a list of inputs.

Besides, Batch Normalization (BN) is a prevalent regularization technique in deep learning, which aims to make the input data of each layer have the same mean and standard deviation, thus mitigates the impact of the intrinsic variance of the data on the network, accelerates training, and prevents overfitting[63]. In this study, the BN layer is applied after the Encoder and Feature Extraction Module, respectively, to normalize the magnitude and dimension of the two feature vectors for the subsequent fusion operation in the Fusion Module.

3. Implementation details and experiments

The training of the deep learning models in this study is based on Tensorflow[64] and Keras[65], using a computation platform with an "Intel Core i7- 4790 @ 3.60 GHz" CPU and a "NVIDIA GeForce RTX 3060" GPU.

3.1. The data set and preprocessing

Wen et al.[12] used OpenSees software to calculate the elastic-plastic time-history responses of 162 typical RC frames under 200 historical ground motions, which is the source of the dataset used in this study. Among them, all the 162 RC frame structures meet the design requirements in China, covering different seismic design intensity (Intensity 6, Intensity 7, and Intensity 8), different number of stories (2, 5, and 8 stories), different story heights (3.3 and 3.9 m), longitudinal column spacing (3.6, 5.4, and 7.2 m), total transverse span (11.7, 13.2, and 16.2 m). In this study, seismic design intensity, number of stories, story height, longitudinal column spacing, and total transverse span are represented as structural information inputs of the following deep learning models. To facilitate the learning and training of the deep learning models, the seismic design intensity is coded according to the one-hot encoding and the rest of the variables are processed according to the Z-Score normalization to eliminate the influence of varied distributions and units. In addition, the acceleration time-history responses of

each floor of the structure are used as the output of the deep learning model, and in order to reduce the dimensionality of the output data, a variable indicating the specific output floor of the building is added to the inputs, which also need to be processed according to the one-hot encoding. More detailed descriptions of the preprocessing of input structural parameters can be found in Table A.1 and Table A.2 of the Supplementary Material.

The ground motions in this dataset are initially selected from the PEER NGA-WEST2 database (https://peer.berkeley.edu/research/data-sciences) based on the magnitude and site conditions, excluding near-fault impulse-type ground motions. Subsequently, 200 ground motions are randomly sampled from the eligible ones, considering magnitudes and PGA, to ensure a diverse and representative representation of ground motion characteristics. The selection criteria and steps for these 200 ground motions are detailed in the paper[12], and their corresponding response spectra are illustrated in Fig. 3. The ground motion series are sampled at a uniform frequency of 50 Hz according to the linear interpolation, and the total durations are unified to 60 s by intercepting or zero-padding to 30 s before and after the peak occurrence moment respectively[12]. Accordingly, the structural nonlinear time history responses corresponding to the processed ground motions are selected as the label value for model training.

The structural nonlinear analyses in this dataset are conducted utilizing the OpenSees software, and the four real buildings discussed in Section 4 are analyzed utilizing the same modeling and analysis methodology. For detailed modeling specifics and validation of correctness, please refer to Section 4.1.

3.2. Data partitioning

The approach adopted in this paper for data partitioning aims to ensure that each dataset comprehensively covers the data characteristics while maximizing the independence of each dataset to avoid data leakage issues. The dataset is partitioned based on the principle of stratified random sampling for the two model inputs: structural parameters and ground-motion time series, as illustrated in Fig. 4. Considering the different number of structural floors (2, 5, and 8 floors) and the different cluster of ground motions (4 classes divided by the k-means cluster analysis), the data sets are divided according to 8:1:1 in each subcategory. The division ratio of training set, validation set and test set in this study is 64 %:17 %:19 % (The corresponding sample counts are 102555, 30480, and 28965, respectively). The details and the effectiveness of this stratified random sampling approach are discussed in Part 2 of the Supplementary Material.

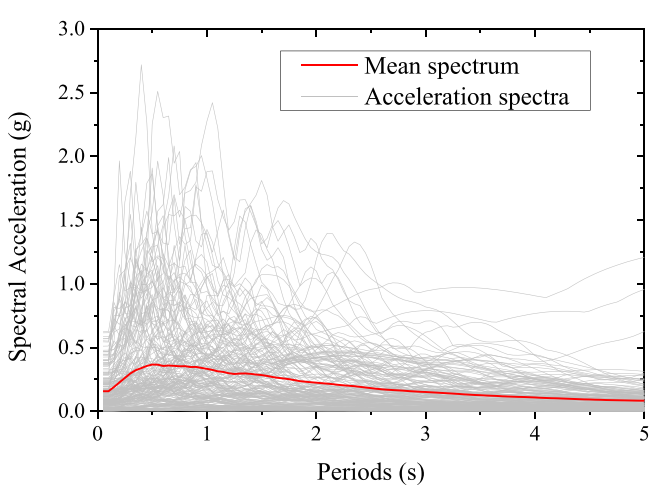

Fig. 3. Acceleration response spectra of selected ground motions [12].

3.3. Evaluation system

3.3.1. Introduction of indicators

In evaluating the prediction effectiveness of time series data, commonly used metrics include dimensional indicators such as mean squared error (MAE), mean absolute error (MSE), root mean squared error (RMSE), dimensionless indicators such as correlation coefficient (r), and coefficient of determination (also known as R2), and confidence intervals (CIs) [30] calculated given the probability density function (PDF) of the normalized error distribution. Moreover, there are some indicators that combine physical significance to analyze the ground motion series and structural response time histories, including the acceleration response spectra, the signal-to-noise ratio (SNR), the arias intensity (AI), and the amplitudes of the seismic time-history responses, e.g., peak floor acceleration (PFA) and maximum inter-story drift ratio (MIDR).

Considering the physical significance of structural time history responses, this paper evaluates the performance of the model proposed in this paper from several perspectives, including common evaluation metrics for regression problems, physical significance indicators, and frequency domain metrics characteristics. The selected evaluation indicators are shown below, and the equations for calculating the relevant indicators are listed in Table A.7 of the Supplementary Material.

1. Time domain evaluation indicators: MSE, R2, SNR, and r
2. Frequency domain evaluation indicators: MSE, R2, SNR, and r
3. Physical indicators: AI (MSE, relative error, and R2), and PFA (MSE, relative error, and R2)

3.3.2. Multi-indicator comprehensive evaluation

Considering that the 14 indicators evaluate the models from different dimensions and perspectives, this paper compares the performance of different models and selects the best model by ranking and scoring each indicator further. The specific procedures are as follows:

1. Determine the range and number **N** of the models to be compared.
2. For each indicator, the actual values of models to be compared are ranked in order of merit, with positive indicators (where larger values indicate better results, e.g., SNR and R2) ranked from largest to smallest, and negative indicators (where larger values indicate worse results, e.g., MSE and relative error) ranked from smallest to largest. For a model ranked k, the score of the model is **Score** $= \mathbf{N} + 1\text{-}k$. The higher the ranking, the higher the score. In terms of any one indicator, the highest score of the model is **N**, and the lowest score of the model is 1.
3. The scores of the 14 indicators of each model are directly summed as the final score, and ranked from best to worst as 1, 2, 3…

The method is simple and easy to use, does not require artificially determined comparison criteria, and is determined only by the relative position of the evaluation unit in the aggregate. It is sufficient to select the best model among a bunch of models.

3.4. Model performance optimization

Different choices of hyperparameters have a significant impact on the performance of the network, so this section focuses on comparison of both training parameters and network architecture hyperparameters. Selecting the optimal parameter in each comparison and then proceeding to compare the next item is the strategy employed to optimize the model's performance in this paper.

3.4.1. Comparison of training hyperparameters

The nonlinear learning ability of deep learning networks comes from the nonlinearity of the activation function, however, the appropriate activation function for different problems varies. For the activation

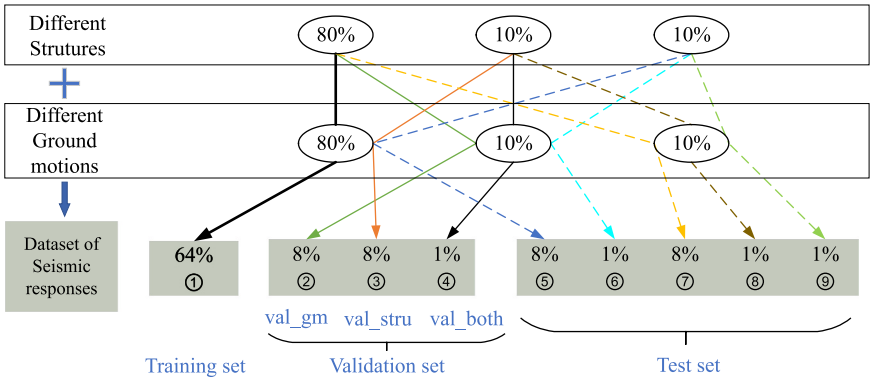

Fig. 4. Schematic diagram of the data set division.

functions, Rectified Linear Unit (ReLU) [66], Leaky ReLU [67], Exponential Linear Unit (ELU) [68] (alpha takes the values of 0.5, 1.0, and 2.0 respectively here), Scaled Exponential Linear Unit (SELU) [69], and Hyperbolic Tangent (Tanh) [70] are compared here. The detailed performance of the network on the validation set using different activation functions is shown in Table A.8 and Table A.9 of the Supplementary Material. On balance, Leaky ReLU has a better performance, which is used in all the models below.

Adam optimizer [71] is widely used in the field of deep learning, where the learning rate is an important parameter. Here, based on the LeakyReLU activation function, three different learning rates are compared: 0.01, 0.001, and 0.0001, and the relevant performances are shown in Table A.10 and Table A.11 of the Supplementary Material, which shows that the best performance is obtained when the learning rate is taken as 0.001. The default learning rate of the following networks is taken as 0.001.

3.4.2. Comparison of fusion operations

Several widely used fusion operations are compared in Table 2, including add fusion operation used in ResNet [72] and feature pyramid network (FPN) [73], multiply fusion operation that has been used to perform fusion of image feature matrices and text feature matrices [74], dot product operation that has been used to capture correlations present in feature maps [75], and concatenation fusion operation that has been used to fuse the structural information vector and the ground motion series vector [12]. The results show that add and subtract have the worst performance, multiply, concatenate and dot have good performance, with concatenate corresponding to the best overall performance.

3.4.3. Comparison of the network backbone architecture

The depth of the network has an important impact on the prediction performance [59]. The schematic diagram of the Encoder is shown in Fig. 5, in which the Encoder is divided into n blocks, and each block contains m convolutional layers and activation functions, and the last layer of each block contains a downsampling operation.

This part compares the effects of using different number of blocks (4, 5, and 6, respectively) and different number of convolutional layers in blocks (1, 2, and 3, respectively) on the network performance based on the base model (using concatenate fusion operation, kernel size=5). The corresponding network performances are shown in Table 3, and it can be seen that increasing the number of blocks and layers can increase the complexity of the network, but not necessarily improve the prediction performance of the network. In this study, the overall performance of "5blocks1layer" is the best under the network design idea and practice.

For convolutional networks, the size of the convolutional kernel also affects the feature extraction effect and computational complexity. The performances of networks with convolutional kernel sizes of 3, 5, 7, 9, and 11, respectively, are shown in Table 4. The results show that the network performs best in the time domain when the kernel size is 11, but the performances on the frequency domain and the physical indicator are mediocre. The smaller convolutional kernel size (like 3 and 5) performs better than the larger convolutional kernel size (like 13 and 15), and the overall performance achieves best when the kernel size is 3.

3.4.4. Comparison of output approaches

To improve the utilization of feature map information at different scales, the adaptive multilevel fusion output is proposed, and the output architecture used in the Decoder is shown in Fig. 6. In this case, the transposed convolution layer is utilized to adjust the dimensionality before transitioning from each layer of the backbone network to the adaptive weighted output.

Taking the Decoder with 5 blocks as example, this part uses 5 adaptive weighting coefficients to linearly weight the outputs of the 5 levels correspondingly, in four types:

Type 1. Only the final features are output. In this case, $w5 = 1$ and the remaining parameters are zero, which is the most common case of direct output.

Type 2. Direct summation of features at each level. In this context, $w1 = w2 = w3 = w4 = w5 = 1$.

Type 3. Five adaptive coefficients of each level features are weighted together. At this point, $w1$, $w2$, $w3$, $w4$, and $w5$ are scalars, which are determined by network training, and the initial values are all taken as 1.0.

Type 4. Five adaptive vectors are weighted for each level feature. In such a situation, $w1$, $w2$, $w3$, $w4$, and $w5$ are all vectors of dimension (3000, 1), where the element values of vectors are optimized through the network training process, and the initial values are all taken as 1.0.

The four output modes are trained separately, and the computed

Table 2
Comparison of different fusion operations for the base model.

Fusion operations	Time domain performance ranking	Frequency domain performance ranking	Physical indicator performance ranking	Overall performance ranking
add	2	4	5	4
subtract	2	5	4	5
multiply	2	2	3	2
concatenate	**1**	**1**	**2**	**1**
dot	5	2	1	3

Note: Due to the length of the paper, only the rankings are listed here. The detailed indicators of the models are shown in Table A.12 of Supplementary Material.

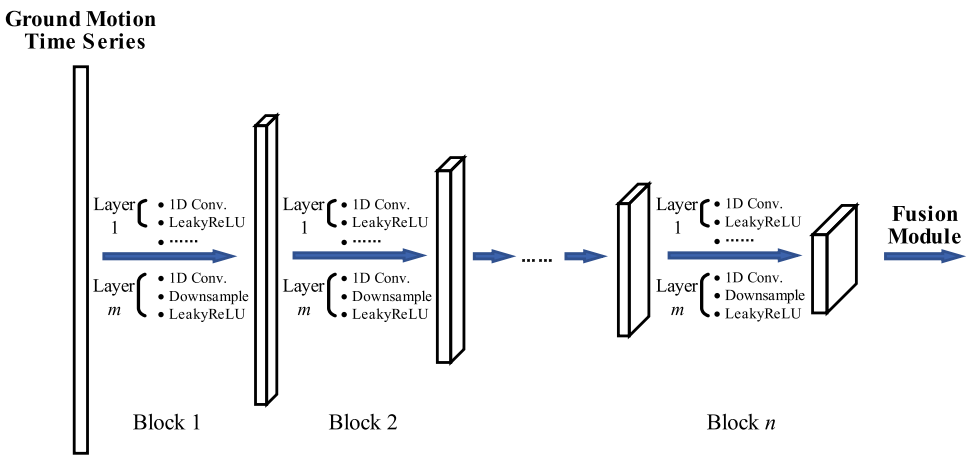

Fig. 5. The schematic diagram of the Encoder.

Table 3
Network performances corresponding to different network structures.

Setting	Number of parameters	Time domain performance ranking	Frequency domain performance ranking	Physical indicator performance ranking	Overall performance ranking
4blocks1layer	266,126	4	4	2	3
4blocks2layer	320,766	5	3	1	2
4blocks3layer	375,406	3	2	4	4
5blocks1layer	**506,099**	**1**	**1**	**3**	**1**
5blocks2layer	724,835	2	5	5	5
5blocks3layer	943,570	7	9	9	9
6blocks1layer	1170,917	6	7	7	6
6blocks2layer	1958,669	8	6	6	7
6blocks3layer	2746,421	8	8	8	8

Note: Due to the length of the paper, only the rankings are listed here. The detailed indicators of the models are shown in Table A.13 of Supplementary Material.

Table 4
Network performance for different kernel sizes.

Kernel size	Number of parameters	Time domain performance ranking	Frequency domain performance ranking	Physical indicator performance ranking	Overall performance ranking
3	**430,563**	**4**	**1**	**1**	**1**
5	506,099	2	2	2	2
7	581,635	5	3	2	4
9	657,171	5	7	4	6
11	732,707	1	4	5	3
13	808,243	3	5	6	5
15	883,779	7	6	7	7

Note: Due to the length of the paper, only the rankings are listed here. The detailed indicators of the models are shown in Table A.14 of Supplementary Material.

results are shown in the Table 5. Type 4 has the most generality and the greatest potential, performing best in both the time and frequency domains. However, Type 3, which reduces the degrees of freedom of the adaptive vectors compared to Type 4, achieves the best overall performance. Consequently, Type 3 is selected as the final strategy. In addition, the use of adaptive weighted fusion performs better than the direct output of the final features or the direct summation of features at all levels.

3.5. Analysis of prediction performance on the test set

This section provides an in-depth performance analysis of the optimized model from the comparisons in Section 3.4, considering the different degrees of elastic-plasticity of the samples in the test set. In accordance with the thresholds of RC frame structures for structural collapse and entry into nonlinearity in FEMA 356[76], the samples in the test set are segregated into the elastic, elastic-plastic, and strongly nonlinear datasets based on the value of IDR, which are shown in Table 6.

The overall performances of the optimized model on these three types of datasets are compared in Table 7, which shows that the overall prediction performance of the model decreases sequentially from the elastic dataset, the elastic-plastic dataset to the strongly nonlinear dataset. Due to the complexity of the time series forecasting problem, it can be seen from the rankings of evaluation results that the time domain performance is not consistent with the frequency domain performance and the performance of the physical indicators, which confirms the need for comprehensive evaluation of the time-series prediction performance from multiple perspectives on the other side.

Some key predictive performances of the optimized model on the test set are depicted in Fig. 7. Observing the histograms illustrating the distribution of correlation coefficients, the optimized model exhibits normal distribution characteristics with similar median values across all three datasets, and the strong nonlinear data set exhibits the highest median value of correlation coefficient (0.687). Regarding the prediction performance of physical indicators (AI and PFA), the energy and amplitude of the predicted time series responses tend to be smaller than the true values, indicating a potential area for improvement in future

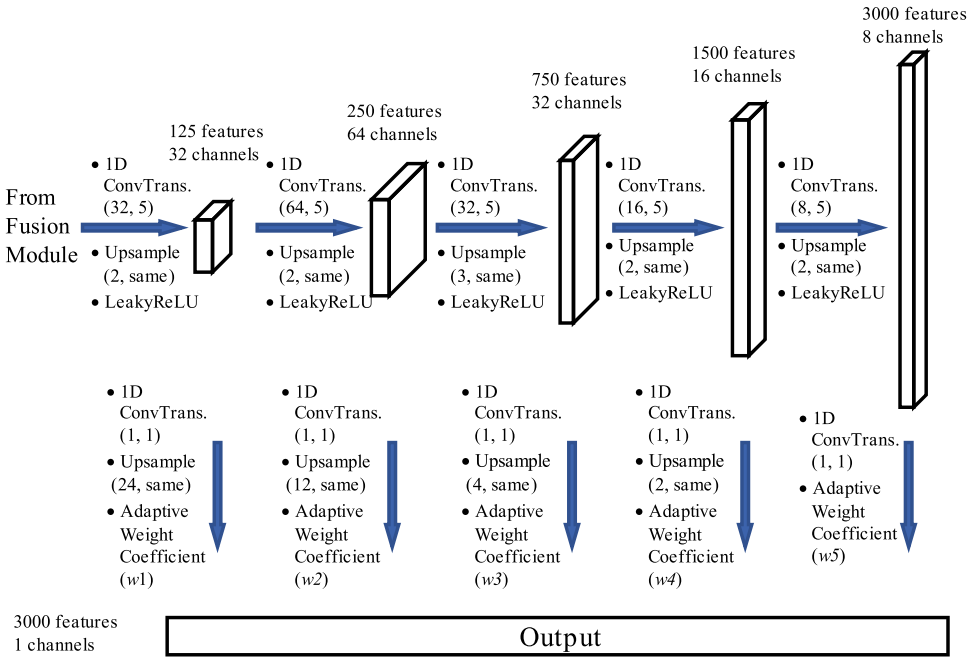

Fig. 6. The architecture of adaptive multilevel fusion output (with 5 blocks as an example).

Table 5
Network performance using different output modes.

Output modes	Number of total model parameters	Time domain performance ranking	Frequency domain performance ranking	Physical indicator performance ranking	Overall performance ranking
Type 1	414,688	3	3	4	4
Type 2	414,932	4	4	2	3
Type 3	**414,937**	**2**	**2**	**1**	**1**
Type 4	429,932	1	1	2	2

Note: Due to the length of the paper, only the rankings are listed here. The detailed indicators of the models are shown in Table A.15 of Supplementary Material.

Table 6
The numbers of examples in different degrees of elasticity and plasticity on the test set.

Dataset	Counts
Elastic dataset ($IDR \leq 0.01$)	24,983
Elastic-plastic dataset ($0.01 < IDR < 0.04$)	3662
Strongly nonlinear dataset ($IDR \geq 0.04$)	320

iterations of the model.

3.6. Comparison with two other types of neural networks

The existing research introduced in the introduction regarding the prediction of structural seismic time-history responses does not integrate building parameters as inputs into the models, which renders them unsuitable for direct comparison with the performance of our model in this paper. Considering that commonly used network architectures in these papers include DNN, CNN, and LSTM, this section additionally proposes and compares the performance of network models based on DNN and LSTM within the autoencoder (AE) framework (shown in Fig. 8). The primary components of these two models are outlined in Table 8, while detailed architectures are illustrated in Figures A.12 of the Supplementary Material.

The two comparison models, along with the optimized model mentioned earlier, are trained using the same training set. Their performance on the identical test set is compared as depicted in Table 9 and Table 10. It is evident that the optimized model outperforms the other two models significantly, whether in the time domain, frequency domain, or physical metrics.

4. Case study

To further analyze the applicability and effectiveness of the proposed model in practical scenarios, this section selects four real structures and twenty historical earthquake records. Using the seismic responses obtained from fine finite element models based on detailed drawings as a reference, a comparative assessment is carried out between the proposed

Table 7
Prediction performance of the optimized model in different degrees of elasticity and plasticity on the test set.

Dataset	Time domain performance ranking	Frequency domain performance ranking	Physical indicator performance ranking	Overall performance ranking
Elastic dataset	2	1	1	1
Elastic-plastic dataset	2	2	2	2
Strongly nonlinear dataset	1	3	3	3

Note: Due to the length of the paper, only the rankings are listed here. The detailed indicators of the models are shown in Table A.17 of Supplementary Material.

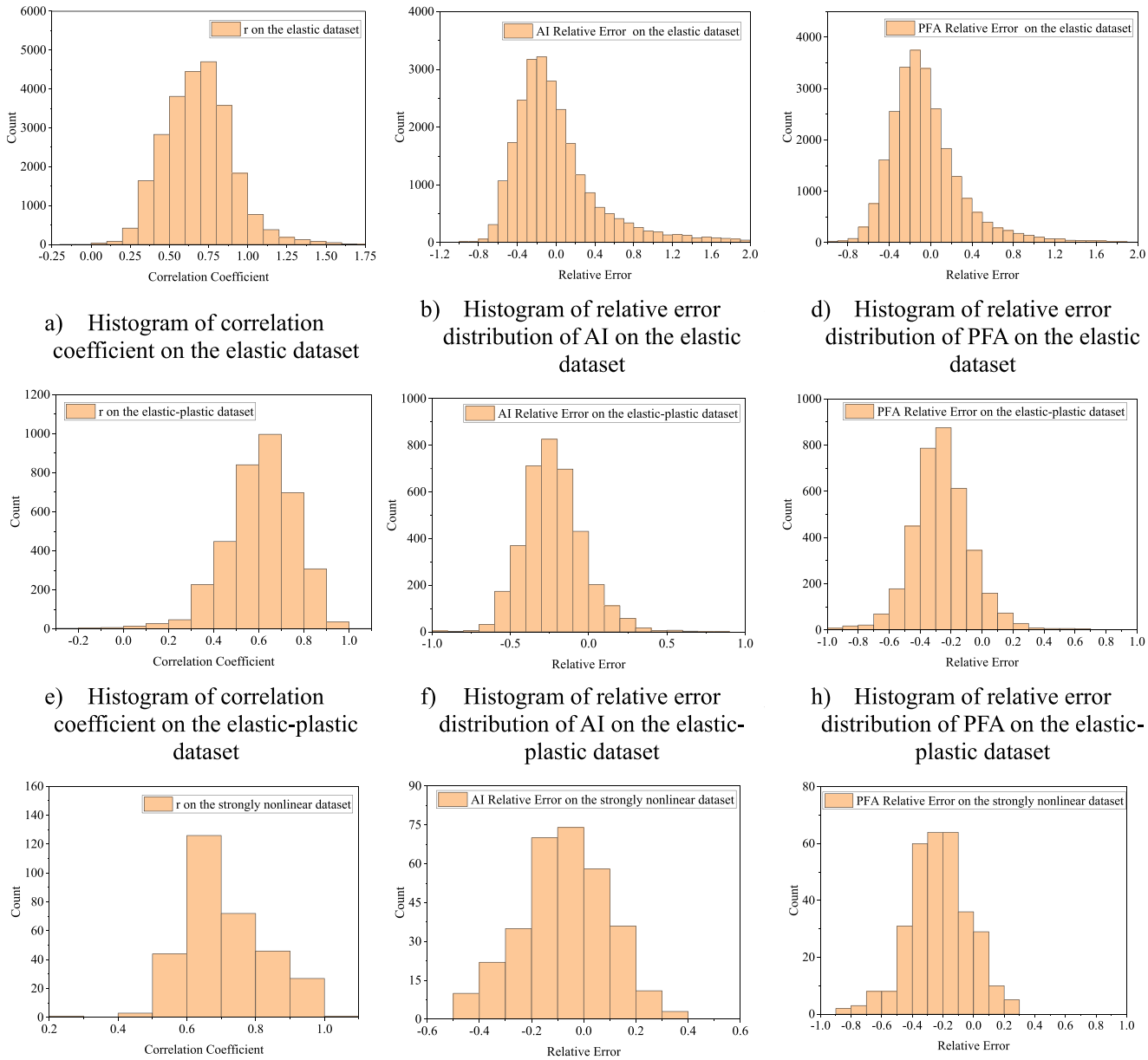

a) Histogram of correlation coefficient on the elastic dataset

b) Histogram of relative error distribution of AI on the elastic dataset

d) Histogram of relative error distribution of PFA on the elastic dataset

e) Histogram of correlation coefficient on the elastic-plastic dataset

f) Histogram of relative error distribution of AI on the elastic-plastic dataset

h) Histogram of relative error distribution of PFA on the elastic-plastic dataset

i) Histogram of correlation coefficient on the strongly nonlinear dataset

j) Histogram of relative error distribution of AI on the strongly nonlinear dataset

l) Histogram of relative error distribution of PFA on the strongly nonlinear dataset

Fig. 7. Performance of the optimized model on datasets with different degrees of elasticity and plasticity. Due to the length of the paper, the more detailed performance analysis of the optimized model is shown in Figure A.9 to Figure A.11 of Supplementary Material.

model in this study and the simplified multi-degree-of-freedom model (referred to as the "simplified MDOF"), which is widely used in seismic analysis of urban-scale buildings. The parameter calibration of the multi-degree-of-freedom model is based on the widely applied method proposed by Lu and Guan[77].

4.1. Description of target buildings

Four well-designed actual structures are selected in this section, and the basic information is shown in the Table 11. These structures are significantly different in terms of number of stories, story height, longitudinal column spacing, and transverse span compared to the aforementioned training samples.

Twenty ground motions are randomly selected from the PEER database, and these samples are independent of the 200 ground motions used to train the models. The lists and response spectra of these earthquakes are shown in Table A.23 and Figure A.15 of Supplementary Material, separately.

The fine finite element models are calculated in OpenSees software (http://opensees.berkeley.edu). For these regular RC frame cases, the Concrete02 material model[78] is employed to simulate concrete, considering both tensile strength and linear tension softening, while the Steel02 material model[79] with the Giuffre-Menegotto-Pinto constitutive relation is used to simulate the reinforcement. Fiber sections are defined for beams and columns. The beams and columns employee nonlinear Beam-Column Elements (also known as Force-Based Beam--Column Elements in OpenSees)[80]. Each beam is discretized into three integration points, while each column has five integration points.

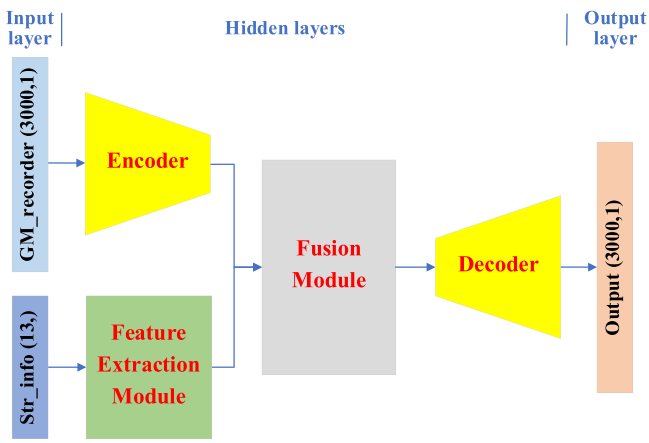

Fig. 8. The AE framework used in this study.

P-Delta effects are considered only in columns, and beams are subjected to linear transformation. The Rayleigh proportional damping model is implemented, with a damping ratio of 5 % assigned to the predominant vibration modes. The dead and live loads are determined in accordance with relevant provisions of the Chinese load code[81]. Additionally, corresponding computational models are established in SAP2000, and the results of the first natural frequency are compared, as shown in Table 12. The errors in the first natural frequency of the buildings between the two software packages do not exceed 5 %, which validates the correctness of the fine finite element models to some extent.

4.2. The prediction performance on these cases

4.2.1. Overall performance analysis

The overall performances of the proposed model and simplified MDOF model on all samples here are compared in Fig. 9, and the detailed performance indicators can be seen in Table A.18 of the Supplementary Material, respectively. The correlation coefficient and coefficient of determination, respectively, indicate the degree of linear correlation in the fitting results and the quality of data fitting by the model. As illustrated in Fig. 9a) and b), it is evident that the performance of the proposed model exhibits greater concentration, fewer significant outliers, and notably superior predictive capabilities in the time domain when compared to the simplified MDOF model. The histogram of confidence level (CL) within 10 % relative error is used to better illustrate the prediction error of time series, and the calculation method is listed in Table A.7 of Supplementary Material. The results presented in Fig. 9c) demonstrate that the proposed model possesses better accuracy and reliability.

Besides, the performances of the optimized model in predicting physical indicators on these cases are shown in Fig. 10. From the scatter plots of physical indicators in Fig. 10 a) and b), it is evident that the time histories predicted by the model in this study exhibit a higher level of accuracy and can effectively capture the computational characteristics of the fine finite element models. From the relative error histograms of physical indicators in Fig. 10 c) and d), the prediction errors of the proposed model are predominantly concentrated within the range of −0.5 to 0, with all errors falling between −1 and 1. In contrast, the simplified MDOF model yields a more dispersed error range and a larger overall error.

4.2.2. Further analysis of three samples

To further elucidate the disparities in predictive performance between the two methods, three samples are randomly selected from seismic responses of different floors for the four buildings subjected to the twenty earthquake records. Some of the computational indicators are shown in Table 13, which shows that in the time-frequency domain,

Table 10
Performance comparison of the three models in terms of the physical indicators.

Type	AI			PFA		
	MSE	R2	relative error	MSE	R2	relative error
Optimized model	0.266	0.697	0.115	0.971	0.436	0.131
AE (DNN)	1.219	−0.230	−0.892	2.333	−0.356	−0.702
AE (LSTM)	0.931	0.060	0.946	1.973	−0.147	0.268

Table 11
Basic information of four cases.

No.	Building 1	Building 2	Building 3	Building 4
Occupancy type	Hotel	Hospital Outpatient Building	Classroom	Office
Construction time	2005	1999	1988	2010
Seismic design intensity	6	7	8	7
Number of stories	7	5	3	6
Story height (m)	3.3	3.6	3.9	3.6
Longitudinal column spacing (m)	4.5	5.1	6.6	7.5
Transverse total span (m)	12.3	13.8	14.7	19.5
Beam cross-section (mm)	250 × 500	250 × 550	250 × 600	250 × 800
Column cross-section (mm)	500 × 500	550 × 550	550 × 550	650 × 650
Concrete strength grade	C35	C35	C35	C35

Table 12
Comparison of first natural periods of the four cases using detailed finite element models.

	Building 1	Building 2	Building 3	Building 4
OpenSees (s)	1.102	0.818	0.543	0.941
SAP2000 (s)	1.093	0.825	0.570	0.936
Relative error	−0.8 %	0.9 %	5.0 %	−0.5 %

Table 8
The primary components of two comparative models based on DNN and LSTM within the AE framework.

	Encoder	Feature Extraction Module	Fusion Module	Decoder
AE (LSTM)	LSTM (2 layers)	Dense (3 layers)	Concatenate layer & Dense (2 layers)	LSTM (2 layers)
AE (DNN)	Dense (3 layers)	Dense (2 layers)	Concatenate layer & Dense (2 layers)	Dense (3 layers)

Table 9
Performance comparison of the three models in both the time domain and the frequency domain (on the same test dataset).

Type	In the time domain				In the frequency domain			
	MSE	SNR	r	R2	MSE	SNR	r	R2
Optimized model	0.038	3.703	0.673	0.392	1.522	2.341	0.797	0.553
AE (DNN)	0.062	3.533	0.104	0.112	7.703	1.542	0.088	−1.697
AE (LSTM)	0.050	3.679	0.619	0.019	5.697	1.841	0.657	−1.224

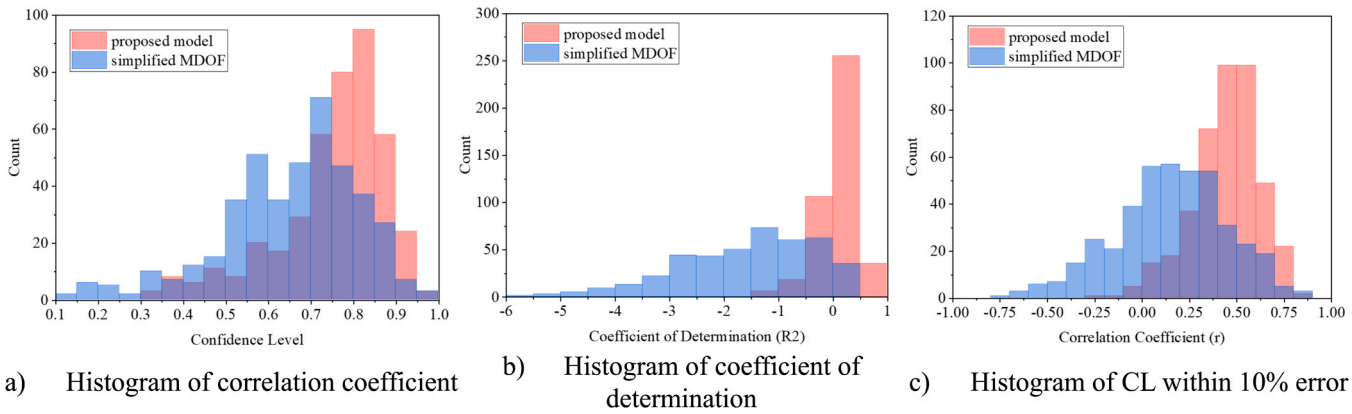

Fig. 9. Prediction performance of the proposed model and simplified MDOF on the cases.

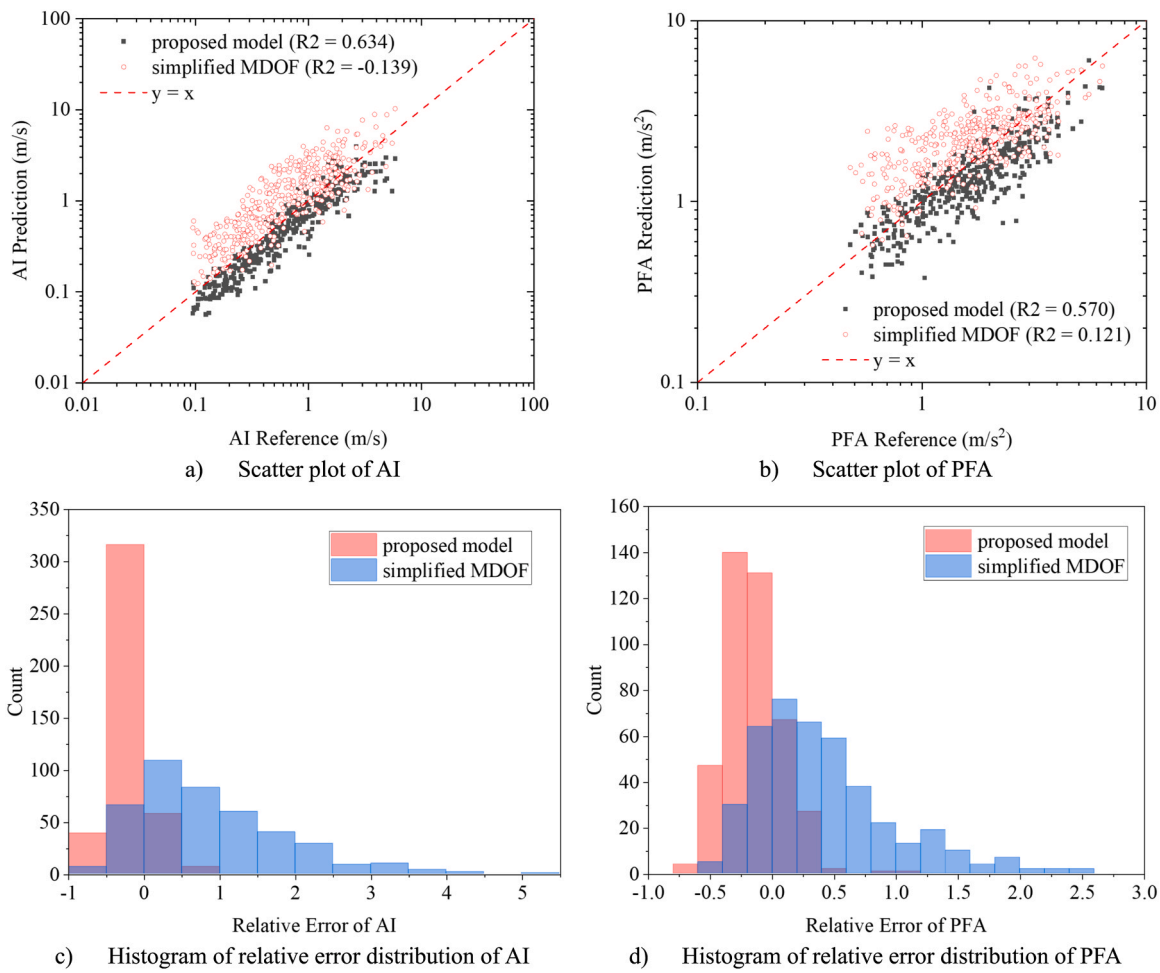

Fig. 10. Prediction performance of the proposed model and simplified MDOF on the cases in terms of the physical indicators.

Table 13
Performance indicators of the proposed model and the simplified MDOF on three samples.

Samples	**Indicators in the time domain**		**Indicators in the frequency domain**		**Physical indicators**	
	MSE	correlation coefficient	MSE	correlation coefficient	relative error of PFA	relative error of AI
No. 15 by proposed model	**0.068**	**0.529**	**0.555**	**0.836**	−0.121	−0.258
No. 15 by simplified MDOF	0.130	0.239	7.782	0.026	0.643	−0.216
No. 348 by proposed model	**0.037**	**0.606**	**1.381**	**0.668**	−0.426	−0.198
No. 348 by simplified MDOF	0.072	0.623	1.590	0.459	−0.236	0.399
No. 411 by proposed model	**0.032**	**0.324**	**1.064**	**0.620**	−0.084	−0.248
No. 411 by simplified MDOF	0.110	−0.268	3.850	0.371	0.107	1.215

the prediction results of the proposed model are significantly better than those of the simplified MDOF model, and from the perspective of the relative errors of the physical indexes, the proposed model performs better than the simplified MDOF model in general.

The acceleration response time histories of the three samples are presented in Fig. 11. It is evident that the predictions of the proposed model effectively capture the overall trends of the acceleration time history responses. In contrast, the disparities in predictions are notably more pronounced when using the simplified MDOF model.

4.2.3. Time consumption

Timeliness is crucial for structural seismic response prediction, especially during post-earthquake emergencies. On an ordinary desktop computer (an "Intel Core i7- 4790 @3.60 GHz" CPU, without GPU), the optimized model's average time required for structural response prediction, including data pre-processing, is 0.044 s per ground motion for single building. In comparison, with the same computational platform, conducting a time history analysis for each structure subjected to every earthquake record using the detailed finite element model requires an average of 2.65 min, and employing the simplified MDOF model for the same analysis on each structure and earthquake record takes an average of 1.90 s. This indicates that when making structural seismic response predictions during the phase of online inference, the computational time of the proposed prediction model takes only 1/3614 of the detailed finite element analysis and 1/43 of the simplified MDOF analysis. Therefore, the model's high computational efficiency and low computational cost can cater to the need for rapid prediction post-earthquakes and significantly reduce the computational time and cost while predicting possible seismic responses of building complexes before earthquakes.

From the analysis of the case studies, it is evident that compared to the widely adopted MDOF methods, the model proposed in this paper exhibits a pronounced advantage in terms of computational accuracy and efficiency. Furthermore, contrasted with fine finite element models built upon detailed structural information, due to the relatively straightforward accessibility of the structural parameters required for this proposed model, it demonstrates excellent feasibility when conducting urban-scale structural response predictions.

5. Conclusions

In this study, we propose a framework for predicting the structural seismic time-history responses of urban-scale reinforced concrete frames. Subsequently, prediction models based on deep learning, trained using a dataset of seismic responses from typical RC frames, are developed and optimized. These models predict the seismic time-history responses of different floors within buildings by inputting ground motion time series along with five easily obtainable building parameters. Furthermore, the optimized model is tested on four actual structures and

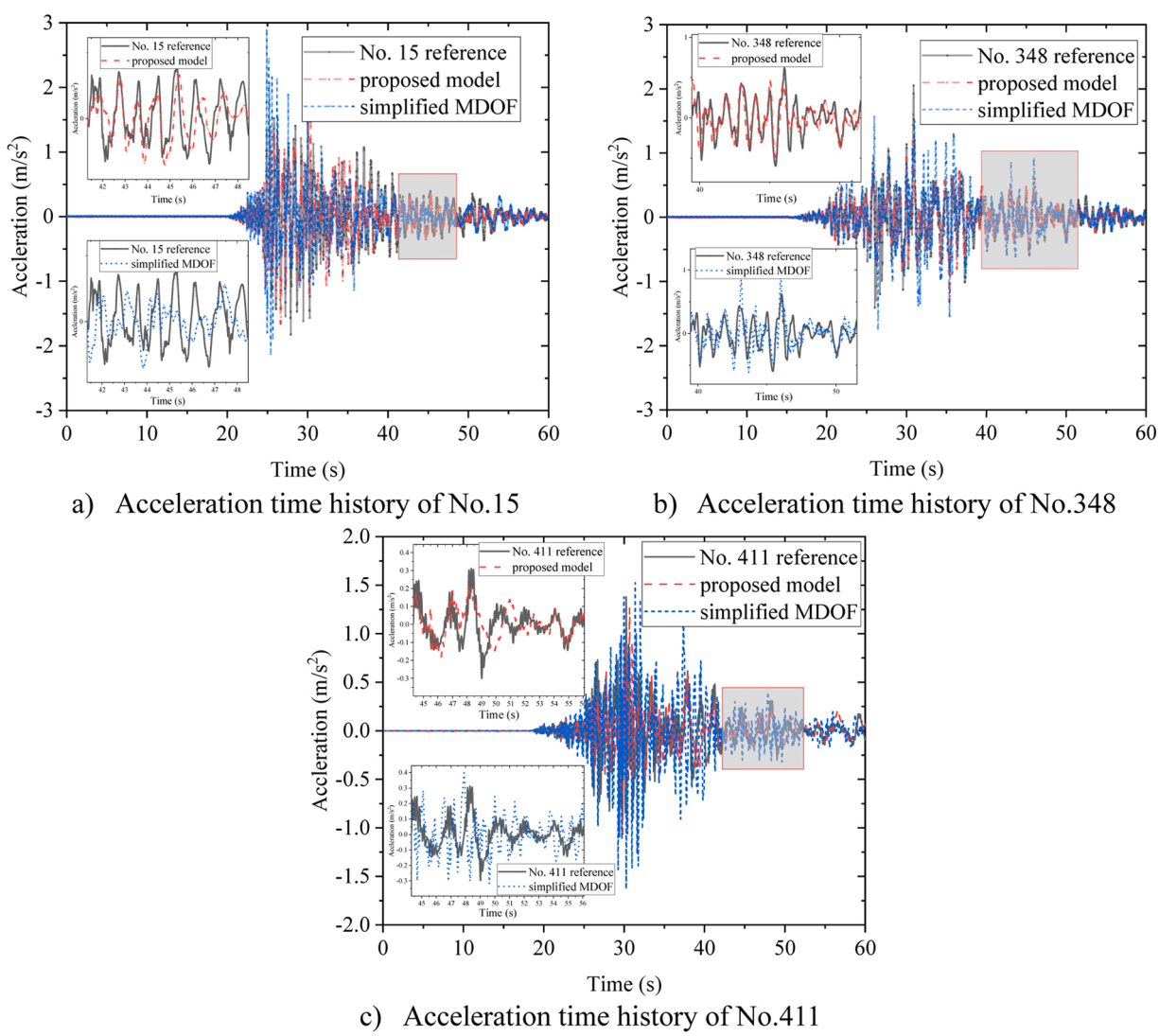

Fig. 11. Prediction performance of the proposed model and simplified MDOF on three samples.

compared with a typical method to further examine its applicability and accuracy. The main conclusions are summarized as follows:

1. A two-stage approach including offline preparation and online inference is proposed to realize rapid prediction of seismic time-history responses of urban-scale buildings. According to this approach, for the RC frame structures, prediction models of seismic time-history responses that take the limited ground motion series and the easy-getting building information as inputs are developed.

2. Considering the complexity of the time-series prediction problem, stratified random sampling during splitting data is employed to prevent data leakage issues, and a comprehensive evaluation system is established from the perspectives of time-frequency domain performance and physical indicators. And drawing on classic works in deep learning, the prediction models with four function modules and the adaptive multi-level fusion output are developed and optimized.

3. The computational accuracy of the proposed model is significantly higher than that of the commonly used simplified MDOF model, and the demand for structural parameters is significantly smaller than that of the detailed finite element simulation. Combined with the high computational efficiency, this model shows a broad application space and strong application value for urban-scale seismic response predictions of RC frames.

The model established in this study still have several limitations. In terms of application scope, the established model does not account for the effects of structural aging or degradation caused by environmental factors. The differences in structural layouts for buildings of different functionalities and their varying seismic resistance capabilities have also not been considered. Due to the composition of the dataset used in this paper and the constraints of model inputs, the model developed herein cannot be applied to high-rise RC frame structures. For irregular RC frame structures, more targeted predictive models need to be developed. Additionally, since the structural seismic response data used in this paper have the same floor height for each structure, the model's applicability is not strictly aligned with buildings with taller ground story height. The predictive performance for such buildings will be evaluated in future urban area case studies.

Author statement

During the preparation of this work, no generative AI and AI-assisted technologies was used. No conflict of interest exists in the submission of this manuscript, and manuscript is approved by all authors for publication. The work described was original research that has not been published previously, and not under consideration for publication elsewhere, in whole or in part.

CRediT authorship contribution statement

Chenyu ZHANG: Writing – review & editing, Writing – original draft, Validation, Software, Methodology, Data curation. **Weiping Wen:** Writing – review & editing, Supervision, Funding acquisition, Conceptualization. **Changhai Zhai:** Supervision, Project administration, Funding acquisition. **Jun Jia:** Investigation, Data curation. **Bochang Zhou:** Resources.

Declaration of Competing Interest

The authors declare that they have no known competing financial interests or personal relationships that could have appeared to influence the work reported in this paper.

Data Availability

Some or all models, data, or code generated or used during the study are available on GitHub (https://github.com/wenwp/StruNet_TH), including the optimized model in this study and the data in Section 4.

Acknowledgements

This investigation is supported by the National Natural Science Foundation of China (No. 52222811 and 52178469), the Fundamental Research Funds for the Central Universities (No. HIT.BRET.2022010), and Natural Science Foundation of Heilongjiang Province (No. LH2021E075). These supports are greatly appreciated.

Appendix A. Supporting information

Supplementary data associated with this article can be found in the online version at doi:10.1016/j.engstruct.2024.118702.

References

[1] Lu X., Jiang Q., Miu Z., Pan P. Elasto-Plastic Analysis of Buildings Against Earthquake. Sanlihe Road, Beijing: China Architecture & Building Press; 2015.
[2] LeCun Y, Bengio Y, Hinton G. Deep learning. Nature 2015;521:436–44.
[3] Raissi M, Perdikaris P, Karniadakis GE. Physics-informed neural networks: a deep learning framework for solving forward and inverse problems involving nonlinear partial differential equations. J Comput Phys 2019;378:686–707.
[4] De Lautour OR, Omenzetter P. Prediction of seismic-induced structural damage using artificial neural networks. Eng Struct 2009;31:600–6.
[5] Morfidis K, Kostinakis K. Seismic parameters' combinations for the optimum prediction of the damage state of R/C buildings using neural networks. Adv Eng Softw 2017;106:1–16.
[6] Morfidis K, Kostinakis K. Comparative evaluation of MFP and RBF neural networks' ability for instant estimation of r/c buildings' seismic damage level. Eng Struct 2019;197:109436.
[7] Hait P, Sil A, Choudhury S. Prediction of global damage index of reinforced concrete building using artificial neural network. Int J Comput Methods Eng Sci Mech 2021;22:386–99.
[8] Hansapinyo C, Latcharote P, Limkatanyu S. Seismic building damage prediction from GIS-based building data using artificial intelligence system. Front Built Environ 2020;6.
[9] Xiong C, Zheng J, Xu L, Cen C, Zheng R, Li Y. Multiple-input convolutional neural network model for large-scale seismic damage assessment of reinforced concrete frame buildings. Appl Sci 2021;11.
[10] Lu X, Xu Y, Tian Y, Cetiner B, Taciroglu E. A deep learning approach to rapid regional post-event seismic damage assessment using time-frequency distributions of ground motions. Earthq Eng Struct Dyn 2021;50:1612–27.
[11] Xu Y, Lu X, Cetiner B, Taciroglu E. Real-time regional seismic damage assessment framework based on long short-term memory neural network. Comput-Aided Civ Infrastruct Eng 2020;36:504–21.
[12] Wen W, Zhang C, Zhai C. Rapid seismic response prediction of RC frames based on deep learning and limited building information. Eng Struct 2022;267:114638.
[13] Arslan MH. An evaluation of effective design parameters on earthquake performance of RC buildings using neural networks. Eng Struct 2010;32:1888–98.
[14] Suryanita R, Maizir H, Jingga H. Prediction of structural response due to earthquake load using artificial neural networks. Int Conf "Engineering Technol, Comput, Basic Appl Sci Ecba Osaka, Jpn 2016.
[15] Gharehbaghi S, Yazdani H, Khatibinia M. Estimating inelastic seismic response of reinforced concrete frame structures using a wavelet support vector machine and an artificial neural network. Neural Comput Appl 2019;32:2975–88.
[16] Nguyen HD, Dao ND, Shin M. Prediction of seismic drift responses of planar steel moment frames using artificial neural network and extreme gradient boosting. Eng Struct 2021;242.
[17] Doran B, Shen JJ, Wen R, Akbas B, Bozer A. Neural network model for seismic response of braced buildings. Proc Inst Civ Eng Struct Build 2017;170:159–67.
[18] Hu J, Wen W, Zhang C, Zhai C, Pei S, Wang Z. Rapid peak seismic response prediction of two-story and three-span subway stations using deep learning method. Eng Struct 2024;300:117214.
[19] Kim T, Kwon O-S, Song J. Response prediction of nonlinear hysteretic systems by deep neural networks. Neural Netw 2019;111:1–10.
[20] Kim T, Song J, Kwon O-S. Probabilistic evaluation of seismic responses using deep learning method. Struct Saf 2020;84.
[21] Kim T, Kwon OS, Song J. Deep learning based seismic response prediction of hysteretic systems having degradation and pinching. Earthq Eng Struct Dyn 2022; 52:2384–406.
[22] Oh BK, Glisic B, Park SW, Park HS. Neural network-based seismic response prediction model for building structures using artificial earthquakes. J Sound Vib 2020;468.
[23] Lagaros ND, Papadrakakis M. Neural network based prediction schemes of the non-linear seismic response of 3D buildings. Adv Eng Softw 2012;44:92–115.
[24] Parida SS, Bose S, Butcher M, Apostolakis G, Shekhar P. SVD enabled data augmentation for machine learning based surrogate modeling of non-linear structures. Eng Struct 2023;280:115600.
[25] Sahoo DM, Chakraverty S. Functional link neural network learning for response prediction of tall shear buildings with respect to earthquake data. IEEE Trans Syst Man Cyber Syst 2018;48:1–10.
[26] Luo H, Paal SG. Artificial intelligence-enhanced seismic response prediction of reinforced concrete frames. Adv Eng Inf 2022;52:101568.

[27] Wu R-T, Jahanshahi MR. Deep convolutional neural network for structural dynamic response estimation and system identification. J Eng Mech 2019;145:04018125.
[28] Oh BK, Park Y, Park HS. Seismic response prediction method for building structures using convolutional neural network. Struct Control Health Monit 2020;27:e2519.
[29] Damikoukas S, Lagaros ND. MLPER: a machine learning-based prediction model for building earthquake response using ambient vibration measurements. Appl Sci 2023;13:10622.
[30] Zhang R, Chen Z, Chen S, Zheng J, Büyüköztürk O, Sun H. Deep long short-term memory networks for nonlinear structural seismic response prediction. Comput Struct 2019;220:55–68.
[31] Xu Z, Chen J, Shen J, Xiang M. Recursive long short-term memory network for predicting nonlinear structural seismic response. Eng Struct 2022;250:113406.
[32] Chou JY, Liu CY, Chang CM. Story drift and damage level estimation of buildings using relative acceleration responses with multi-target deep learning models under seismic excitation. Earthq Eng Struct Dyn 2023;52:2554–71.
[33] Bailey Bond R, Ren P, Hajjar JF, Sun H. Physics-informed machine learning for seismic response prediction of nonlinear steel moment resisting frame structures. arXiv e-prints 2024:17992. arXiv:2402.
[34] Yu Y, Yao HP, Liu YM. Structural dynamics simulation using a novel physics-guided machine learning method. Eng Appl Artif Intell 2020;96:103947.
[35] Torky AA, Ohno S. Deep learning techniques for predicting nonlinear multi-component seismic responses of structural buildings. Comput Struct 2021;252:106570.
[36] Zhang H, Bittner M, Beer M. Seismic response meta-model of high-rise fame structure based on time-delay neural network. KSCE J Civ Eng 2022;26:2273–94.
[37] Wang T, Li H, Noori M, Ghiasi R, Kuok S-C, Altabey WA. Seismic response prediction of structures based on Runge-Kutta recurrent neural network with prior knowledge. Eng Struct 2023;279:115576.
[38] Zhang R, Liu Y, Sun H. Physics-informed multi-LSTM networks for metamodeling of nonlinear structures. Comput Methods Appl Mech Eng 2020;369:113226.
[39] Zhang R, Liu Y, Sun H. Physics-guided convolutional neural network (PhyCNN) for data-driven seismic response modeling. Eng Struct 2020;215:110704.
[40] Sadeghi Eshkevari S, Takáč M, Pakzad SN, Jahani M. DynNet: physics-based neural architecture design for nonlinear structural response modeling and prediction. Eng Struct 2021;229:111582.
[41] Guo J, Enokida R, Li D, Ikago K. Combination of physics-based and data-driven modeling for nonlinear structural seismic response prediction through deep residual learning. Earthq Eng Struct Dyn 2023;52:2429–51.
[42] Zhou Y, Meng S, Lou Y, Kong Q. Physics-informed deep learning-based real-time structural response prediction method. Engineering 2023.
[43] Xiong Q, Kong Q, Xiong H, Liao L, Yuan C. Physics-informed deep 1D CNN compiled in extended state space fusion for seismic response modeling. Comput Struct 2024;291:107215.
[44] Hu Y, Guo W, Xu Za, Shi C. Physics knowledge-based transfer learning between buildings for seismic response prediction. Soil Dyn Earthq Eng 2024;177:108420.
[45] Fan G, Li J, Hao H, Xin Y. Data driven structural dynamic response reconstruction using segment based generative adversarial networks. Eng Struct 2021;234:111970.
[46] Wang T, Li H, Noori M, Ghiasi R, Kuok S-C, Altabey WA. Probabilistic seismic response prediction of three-dimensional structures based on bayesian convolutional neural network. Sensors 2022;22:3775.
[47] Nikolopoulos S, Kalogeris I, Papadopoulos V. Machine learning accelerated transient analysis of stochastic nonlinear structures. Eng Struct 2022;257:114020.
[48] Kim T, Song J, Kwon OS. Pre- and post-earthquake regional loss assessment using deep learning. Earthq Eng Struct Dyn 2020;49:657–78.
[49] Xiong C, Lu X, Lin X, Xu Z, Ye L. Parameter determination and damage assessment for THA-based regional seismic damage prediction of multi-story buildings. J Earthq Eng 2017;21:461–85.
[50] Lu X, McKenna F, Cheng Q, Xu Z, Zeng X, Mahin SA. An open-source framework for regional earthquake loss estimation using the city-scale nonlinear time history analysis. Earthq Spectra 2020;36:806–31.
[51] Hori M, Ichimura T, Maddegedara L. Integrated earthquake simulation. CRC Press,; 2022.
[52] Hori M, Ichimura T. Current state of integrated earthquake simulation for earthquake hazard and disaster. J Seismol 2008;12:307–21.
[53] Mooney P, Minghini M. A review of OpenStreetMap data. London: Ubiquity Press,; 2017.
[54] M.O.H.U.R.D, Seismic Ground motion parameter zonation map of China (GB 18306-2015) 2015 Architecture & Building Press, Beijing, China.
[55] Liang J, Gong J, Li W. Applications and impacts of Google Earth: a decadal review (2006–2016). ISPRS J Photogramm Remote Sens 2018;146:91–107.
[56] Xu ZK, Chen J, Shen JX, Xiang MJ. Regional-scale nonlinear structural seismic response prediction by neural network. Eng Fail Anal 2023;154.
[57] Xu Z, Wu Y, Qi M-z, Zheng M, Xiong C, Lu X. Prediction of structural type for city-scale seismic damage simulation based on machine learning. Appl Sci 2020;10.
[58] The Central People's Government of the People's Republic of China The First National Comprehensive Survey on Natural Disaster Risk Has Been Successfully Completed, Obtaining Data on Disaster Risk Factors Totaling Billions of Records; 2023, https://www.gov.cn/xinwen/2023–02/16/content_5741672.htm. Accessed on 5 March, 2024. (in Chinese).
[59] Goodfellow I, Bengio Y, Courville A. Deep learning. Cambridge: MIT press,; 2016.
[60] Michelucci U. An introduction to autoencoders. arXiv Prepr arXiv 2022:220103898.
[61] Kislov KV, Gravirov VV, Vinberg FE. Possibilities of seismic data preprocessing for deep neural network analysis. Izv, Phys Solid Earth 2020;56:133–44.
[62] Helal EB, Saad OM, Hafez AG, Chen Y, Dousoky GM. Seismic data compression using deep learning. IEEE Access 2021;9:58161–9.
[63] Ioffe S, Szegedy C. Batch normalization: accelerating deep network training by reducing internal covariate shift. Int Conf Mach Learn pmlr 2015:448–56.
[64] Abadi M, Agarwal A, Barham P, Brevdo E, Chen Z, Citro C, et al. Tensorflow: large-scale machine learning on heterogeneous distributed systems. arXiv Prepr arXiv 2016:160304467.
[65] Chollet F. Keras: Deep Learning for Humans. 2015; https://github.com/keras-team/keras/. Accessed on 20 February, 2023.
[66] Nair V, Hinton GE. Rectified linear units improve restricted boltzmann machines. Proc 27th Int Conf Mach Learn 2010;(ICML-10):807–14.
[67] Maas AL, Hannun AY, Ng AY. Rectifier nonlinearities improve neural network acoustic models. Proc 30th Int Conf Mach Learn Atlanta, Ga, USA 2013:1–6.
[68] Clevert D.-A., Unterthiner T., Hochreiter S. Fast and accurate deep network learning by exponential linear units (elus). arXiv preprint arXiv:151107289. 2015.
[69] Klambauer G, Unterthiner T, Mayr A, Hochreiter S. Self-normalizing neural networks. Adv Neural Inf Process Syst 2017:30.
[70] Pineda FJ. Generalization of back-propagation to recurrent neural networks. Phys Rev Lett 1987;59:2229.
[71] Kingma DP, Ba J Adam. A method for stochastic optimization. arxiv prepr arxiv 2014:14126980.
[72] He K, Zhang X, Ren S, Sun J. Deep residual learning for image recognition. Proceedings of. IEEE Conf Comput Vis Pattern Recognit 2016:770–8.
[73] Lin T-Y, Dollár P, Girshick R, He K, Hariharan B, Belongie S. Feature pyramid networks for object detection. Proc IEEE Conf Comput Vis Pattern Recognit 2017:2117–25.
[74] Liao W, Huang Y, Zheng Z, Lu X. Intelligent generative structural design method for shear wall building based on "fused-text-image-to-image" generative adversarial networks. Expert Syst Appl 2022;210:118530.
[75] Vaswani A, Shazeer N, Parmar N, Uszkoreit J, Jones L, Gomez AN, et al. Attention is all you need. Adv Neural Inf Process Syst 2017:30.
[76] American Society of Civil Engineers. Prestandard and Commentary for the Seismic Rehabilitation of Buildings (FEMA 356). Washington, DC.: Federal Emergency Management Agency; 2000.
[77] Lu X, Guan H. Earthquake disaster simulation of civil infrastructures: from tall buildings to urban areas. Singapore: Springer,; 2017.
[78] OpenSeesWiki. Concrete02 Material – Linear Tension Softening. 2010; https://opensees.berkeley.edu/wiki/index.php/Concrete02_Material_–_Linear_Tension_Softening. Accessed on September 1, 2021.
[79] OpenSeesWiki. Steel02 Material – Giuffre-Menegotto-Pinto Model with Isotropic Strain Hardening. 2012; https://opensees.berkeley.edu/wiki/index.php/Steel02_Material_–_Giuffr%C3%A9-Menegotto-Pinto_Model_with_Isotropic_Strain_Hardening. Accessed on September 1, 2021.
[80] OpenSeesWiki. Force-Based Beam-Column Element. 2016; ⟨https://opensees.berkeley.edu/wiki/index.php/Force-Based_Beam-Column_Element⟩. Accessed on September 1, 2021.
[81] M.O.H.U.R.D, Load Code for the design of building structures (GB50009-2012) 2012 Architecture & Building Press, Beijing, China.